Article

A Super Resolution Probe to Monitor HNO Levels in the Endoplasmic Reticulum of Cells

Firoj Ali, Sreejesh Sreedharan, Anila Hoskere Ashoka, Hiwa K. Saeed, Carl G W Smythe, Jim Antony Thomas, and Amitava Das

Anal. Chem., **Just Accepted Manuscript** • DOI: 10.1021/acs.analchem.7b02567 • Publication Date (Web): 26 Oct 2017

A Super Resolution Probe to Monitor HNO Levels in the Endoplasmic Reticulum of Cells

Firoj Ali,[a] *Sreejesh Sreedharan,*[b] *Anila Hoskere Ashoka,*[a] *Hiwa K Saeed,*[b] *Carl G W Smythe,* [c] *Jim A Thomas,*[*b] *Amitava Das*[*a,d]

[a]Organic Chemistry Division, CSIR-National Chemical Laboratory, Pune-411008, India.

[b]Department of Chemistry, University of Sheffield, Sheffield, S3 7HF, UK.

[c]Department of Biomedical Science, University of Sheffield, Sheffield, S10 2TN, UK.

[a,d]CSIR-Central Salt & marine Chemicals Research Institute, Bhavnagar: 364002, Gujarat, India.

ABSTRACT: Selective detection of nitroxyl (HNO), which has recently been identified as a reactive nitrogen species, is a challenging task. We report a BODIPY-based luminescence ON reagent for detection of HNO in aqueous solution and in live RAW 264.7 cells, based on the soft nucleophilicity of the phosphine oxide functionality towards HNO. The probe shows high selectivity to HNO over other reactive oxygen/nitrogen and sulphur species. Luminescence properties of the BODIPY based chemodosimetric reagent make it an ideal candidate for use as a reagent for super resolution structured illumination microscopy. The viability of the reagent for biological *in-vivo* imaging application was also confirmed using Artemia as a model.

Keywords: HNO • luminescence • superresolution imaging • endoplasmic reticulum•

Introduction

Recently, nitroxyl (HNO) has been identified as an enigmatic reactive nitrogen species and a potential pharmacological agent.[1,2] It is thought that HNO is generated from $NO^{\bullet}$ synthases through oxidation of N-hydroxy-L-arginine or via reduction of $NO^{\bullet}$ by mitochondrial xanthine oxidase, cytochrome c.[3] Recent advances in the understanding of the chemistry of HNO reveals that this species displays unique cardiovascular properties.[4,5] It is established that HNO accounts for positive lusitropic and ionotropic effects in failing hearts without a chronotropic effect, and it also causes a release of the neurotransmitters, glutamate, and calcitonin-gene related peptide which modulate calcium channels such as ryanodine receptors.[6] Apart from its beneficial effects in cardiovascular disease, HNO is known to inhibit GAPDH, a key glycolytic enzyme for tumor proliferation and cancer cell apoptosis.[7] Furthermore, studies have also established that HNO interacts with thiol-containing enzymes such as polymerase, aldehyde dehydrogenase,

glyceraldehyde-3-phosphate dehydrogenase, and ADP-ribose to inhibit enzyme activity.[8,9] It also interferes with redox-based immunity mechanisms through fast depletion of glutathione,[10] and is a more efficient platelet aggregation inhibitor compared to traditional nitrovasodilators.[11]

Interestingly, biochemical transformations induced by HNO are significantly different than those induced by NO. The biochemical accumulation of HNO depends on a delicate balance between scavenging and activating/deactivating pathways.[12] HNO, is an electronic singlet, since the generation of the corresponding deprotonated species, $^{3}NO^{-}$ is spin forbidden (its adiabatic singlet-triplet transition energy is 18.45 kcal/mol)[13] HNO is the predominant species (pK_a^{HNO} = 11.4)[14] at physiological pH. Given the diversity of its biological functions- and the fact that HNO rapidly converts to N_2O[15]- fast and specific recognition/estimation of HNO is essential in understanding the biochemical role of HNO in human physiology.[16-18]

Several methodologies based on various analytical techniques such as colorimetric methods, EPR, HPLC, mass spectrometry, and electrochemical analysis, for the detection of HNO are available in the literature.[1,2] Such methodologies are either time consuming or involve the destruction of cells and tissues and are thus not ideally suited to *in-vivo* tracking and detection of HNO. In this context, reagents that show a fluorescence ON response on detection of HNO have an obvious edge for use as an imaging reagent as well as for studying bio-species in living samples. Such reagent also allows high sensitivity and spatiotemporal resolution. Among the various reagents that show such a response, phosphine-based reagents have received considerable attention.[1,2] King and co-workers were first to report the reaction of HNO with organic phosphines to produce the corresponding phosphine oxide and azaylide.[19,20] Since then, chemodosimetric probe molecules have been exploited this reaction for specific detection of HNO using fluorophores like rhodamine, coumarine, napthalimide and BODIPY.[21-29] This

reaction has also been exploited in developing FRET-based receptors for HNO.[30] Most of these receptors show a luminescence response within the visible region of the spectrum. For example, Lippard and co-workers have reported a Cu(II)-complex of a coumarin-derivative that shows specificity towards HNO with a luminescence ON response (λ_{Max} = 625 nm).[31] Unlike most other Cu(II)-based reagents, this reagent shows remarkable specificity towards HNO over L-(+)-cysteine, GSH, or methionine. In related work, Lin and co-workers have used a phosphine based derivative for two-photon imaging of exogenous HNO in HeLa cells following excitation at 780 nm (λ_{Mon} = 512 nm).[32] Despite such efforts, examples of probes for the targeted detection/ scavenging of HNO in specific organelles are rather uncommon, thus there is ample scope for the development of such reagents.

Despite its many attractions, one of the drawbacks of employing optical microscopy is that it has a practical resolution limit of around 250 nm.[33,34] More recently this drawback is being addressed through super resolution microscopy, SRM, in which techniques which break this resolution limit have been developed. A range of SRM methods have been developed; while pointillistic techniques such as STORM and STED produce the highest resolutions, they require long acquisition times, intense laser power, and/or exceptionally stable chromophores. In contrast whilst structured illumination microscopy (SIM) provides imaging with 100 nanometers resolution,[36] its particular advantages is that it makes less demand on the photostability of imaging luminophore and necessitates lower acquisition times; so that, of all the SR techniques, it is most ideally suited to 3-D sectioning.[34] However, as image acquisition in SIM still involves exposure of luminophores to a high-power laser source over an extended time window, effective SIM-compatible probes must show high photostability. In this study, we describe a probe that is suitable for SIM that specifically detects HNO in the ER.

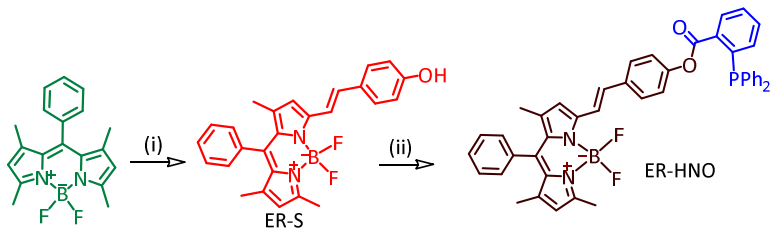

Scheme 1. Methodologies adopted for the synthesis of **ER-HNO**.

Experimental section

All commercial reagents were procured from suppliers, were used as received without further purification. Angeli's salt (AS) was used as HNO donor. Solvents were dried as and when required by using standard procedures. **ER-S** was synthesized as described previously.[36] ^{1}H and ^{13}C NMR spectra were recorded on Bruker 400/500 MHz FT NMR (Model: Advance-DPX 400/500) using TMS as an internal standard. All the Fluorescence measurements were carried out on *PTI* Quanta Master™ Steady State Spectrofluorometer. High-resolution mass spectra were recorded on JEOL JM AX 505 HA mass spectrometer. UV Spectra were recorded using Shimadzu UV-1800 spectrometer. Confocal images were acquired in Olympus Fluoroview Microscope. All the Structured Illumination Microscopy (SIM) experiments and Wide Field Fluorescence Microscopy Experiments were performed by using Delta Vision OMX-SIM (GE Healthcare). The Post-processing SIM reconstructions were performed by using Soft Worx software

General experimental methods for UV-Vis and fluorescence studies:

Stock solution of probe **ER-HNO** (5×10^{-3} M) was prepared in HPLC grade acetonitrile, and the same solution was used for all the studies after appropriate dilution to 5 ml of PBS (pH 7.2) to

make the effective ligand concentration of 10 μM. Unless and otherwise mentioned, 10 mM and pH 7.2 solution of aq. HEPES buffer was used for all spectroscopic studies. All reactive oxygen species and nitrogen species solutions of 1×10^{-3} M were prepared in PBS buffer medium having pH 7.2. All luminescence measurements were done using λ_{Ext} = 530 nm with an emission slit width of 2/2 nm.

Cell-culture and Microscopy experiments:

RAW 264.7 cells were seeded on Coverslips (22 mm X 22 mm, 170 ± 5 μm square Cover glasses) placed in 6 well plates in DMEM culture medium containing (10% FBS and 1% Penicillin Streptomycin) for 24 hours at 37°C, 5% CO_2. After 24 hours when 70% Confluency was achieved the cells were washed with DMEM culture medium then cells were treated with **ER-HNO** probe (1 μM) for 30 minutes. Cells were then washed thrice with culture medium and further treated with different Angeli's salt (AS) for 30 min. After that cells were washed again with Phosphate Buffer Saline (3X PBS). After carrying out the Live cell uptake of the **ER-HNO** probe and the small molecule, the cells were fixed with 4% PFA for 15 min and then washed thrice with PBS and two times and then the coverslips were mounted using the Mounting medium (Vectashield h-1000).The Coverslips were then sealed using Nail varnish and the sample was then imaged. As Structured Illumination Microscopy (SIM) relies on the cell morphology, the cells were examined with a light microscope and then imaged using SIM.

Synthesis

Synthesis of ER-HNO: Under N_2 atmosphere, to a solution of 2-(diphenylphosphino) benzoic acid (100 mg, 0.32 mmol) in dry CH_2Cl_2, DCC (80 mg, 0.39 mmol) was added and stirred at 0^oC for 2hr. To this, Compound **ER-S** (150 mg, 0.35 mmol) and DMAP (20 mg, 0.16 mmol) were added and it was stirred at room temperature for 6 hr. Reaction was monitored by TLC. Then the

mixture was concentrated under vacuum, and the crude product was purified by silica gel column chromatography bu using 5% Ethyl acetate in PET ether medium to give the compound **ER-HNO**. Yield 36%. ^{1}H NMR ($CDCl_3$, 500 MHz, δ ppm, *J* in Hz) : 7.60 (1H, d, *J* = 16.3), 7.53 (2H, d, *J* = 8.6), 7.49 (4H, t, *J* = 5.3), 7.47 – 7.42 (2H, m), 7.33 (10H, dd, *J* = 13.2, 7.2), 7.30 (2H, d, *J* = 7.5), 7.18 (1H, d, *J* = 16.3), 7.03 – 6.98 (1H, m), 6.93 (2H, d, *J* = 8.5), 6.59 (1H, s), 6.01 (1H, s), 2.60 (3H, s), 1.42 (3H, s), 1.39 (3H, s). ^{13}C NMR ($CDCl_3$, 125 MHz): 190.99, 164.54, 155.27, 155.06, 153.99,153.80, 142.51, 141.53, 137.30, 134.76, 134.53,134.15, 133.94, 133.68, 133.48, 133.16,132.88, 132.35, 131.94, 131.85, 131.75, 131.44, 131.11, 130.98, 128.91, 128.67, 128.60, 128.48,128.41, 122.42, 116.15, 25.98. HRMS (ESI): m/z calcd for $C_{45}H_{36}BF_2N_2O_2P$ [M+H]: 716.5756, found 717.2849.

Results and Discussion

The methods used to synthesize probe and characterize **ER-HNO** and its luminescent partner **ES-S** are shown in scheme 1. This probe exploits the use of phosphine derivative for specific recognition of HNO and relies on a reductive ligation process. The phosphine functionality reacts with HNO to produce an intermediate azaylides, leading to cleavage of the 2-diphenylphosphino)benzoate moiety.[37-39] As mentioned earlier, HNO exists solely at pH 7.2. Electronic spectrum recorded for **ER-HNO** and band maxima were observed at 562 nm in PBS-CH_3CN (9:1,v/v) buffer medium and this was attributed to a S0 →S1 transition (SI). Following excitation at 530 nm, Reagent **ER-HNO** showed a weak emission band (Φ= 0.002, for λ_{Ext}= 530 nm) with maxima at 570 nm under identical experimental condition. The reaction of **ER-HNO** with HNO generated by Angeli's salt[40] leads to the generation of the corresponding derivative of the BODIPY moiety (**ER-S**) which has an appreciably higher emission quantum yield.

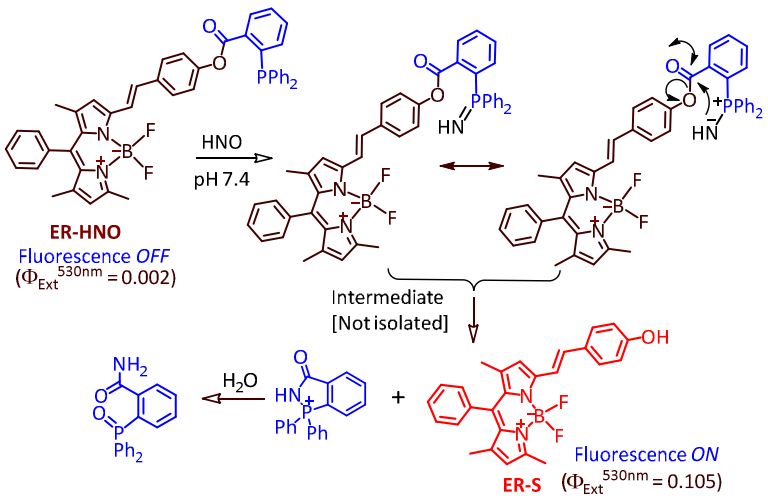

Scheme 2: **ER-HNO** releases emissive BODIPY derivative **ER-S** when exposed to HNO.

This enhancement in emission response can be exploited to detect and quantify HNO in PBS-CH_3CN (9:1,v/v) buffer medium under physiological conditions (pH 7.2). Formation of **ER-S** as the reaction product of **ER-HNO** was also confirmed by ESI-MS. A systematic emission titration of **ER-HNO** with increasing concentrations of HNO revealed a gradual increase in solution emission with subsequent generation of **ER-S** (Figure 1B) accompanied by the generation of a new emission band at a maximum at λ_{Max}= 586 nm (Φ = 0.105, for λ_{Ext}= 530 nm). A good linear relationship between emission intensity and concentration of HNO in the range of 2 - 15 μM is observed (SI) and its detection limit was found to be 2 μM (SI). To examine the selectivity of the probe, we performed *in-vitro* tests incubating **ER-HNO** (10 μM) with other RNS and ROS species (100 μM of AS and 200 μM of HOCl, H_2O_2, OH, NO_3^-, NO_2^-, Cys, GSH, NO, $ONOO^-$ and S^{2-}) (SI) in PBS-CH_3CN (9:1,v/v) buffer medium. The resultant emission spectra, recorded in PBS, are shown in Figure 1.

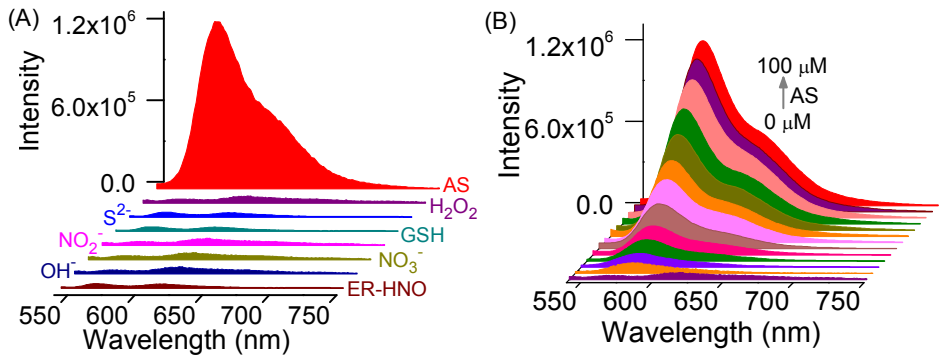

Figure 1. (A) Change in emission of **ER-HNO** solution (10 μM) in the absence and presence of different analytes (0.1 mM of AS and 0.2 mM; HOCl, H_2O_2, $^{\cdot}OH$, NO_3^-, NO_2^-, Cys, NAC, GSH and S^{2-}; (B) emission titration profile on varying [AS] (0–100 μM).Studies were performed in aq. PBS buffer–CH_3CN (9:1, v/v; pH 7.2) medium; $\lambda_{Ext}/\lambda_{Em}$: 530/585 nm.

Except for HNO, which induces the expected turn ***ON*** emission response, no significant change in emission intensity is observed in the presence of any other RNS and ROS species. Even other potential anionic and cationic analytes, as well as biologically relevant thiols (Cys, GSH, and NAC), under the identical experimental condition, failed to show any such change (SI). The results of these interference studies also reveal that the emission response of **ER-HNO** in the presence of 10 mole equivalent of AS remains unchanged in the presence of even higher concentrations of the other analytes mentioned above (SI). These results confirm that the probe molecule **ER-HNO** is specific towards HNO. Further studies also reveal that the emission spectrum of **ER-HNO** remains unchanged over a wide range of pH 4-10 (SI).

This distinctive emission response under physiological condition, as well as its specificity to HNO, led us to examine the toxicity of the probe molecule towards live RAW 264.7 macrophages cells and cytotoxicity assays confirmed the low toxicity of the probe (SI). This encouraged us to explore the use of the probe as an imaging reagent for the intracellular

detection of HNO in these macrophage cells. Cells in DMEM culture media were incubated with **ER-HNO** (1.0 μM) for 15 minutes at 37 °C and subsequently viewed under confocal laser scanning microscope (CLSM) using a 530 nm laser as an excitation source. No intracellular fluorescence was observed until these pre-treated cells were also exposed to AS, then a strong intracellular fluorescence was observed under CLSM (Figure 2).

High emission quantum yield, photostability and non-toxicity are primary important factors for a reagent to be used for the super resolution microscopy (SRM) technique, SIM. Unarguably SIM is one of the most attractive SRM imaging techniques. However, image acquisition involves exposure of luminophores to a high power laser source over an extended period of time windows, thus SIM compatible probes must show high photostability and low bleach rates. Given the photophysical properties of ER-HNO, its compatibility with SIM was also investigated.

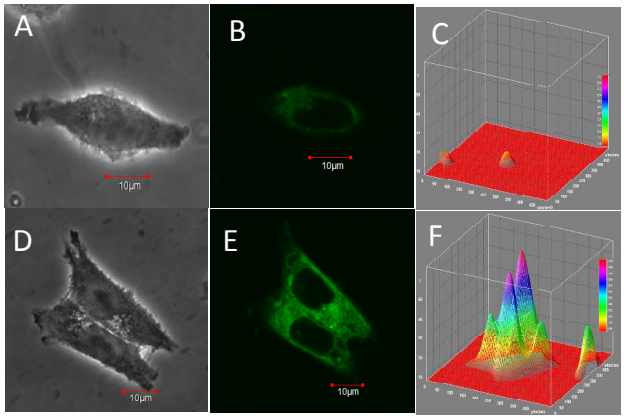

Figure 2. (A–C) Confocal laser scanning microscopic (CLSM) images of RAW 264.7 cells incubated with **ER-HNO** (1 μM) as the control: (A) bright field; (B) dark field laser and (C) 3D intensity plot of image (B); (D–F) CLSM images of cells incubated with **ER-HNO** (1 μM) for 15 min and then further exposed to AS (20 μM) for 20 min at 37 ^{0}C: (D) bright field; (E) dark field laser; (F) 3D intensity plot of image (E). $\lambda_{Ext}/\lambda_{Em}$ = 530/573 nm.

As for the CLSM experiments, RAW macrophage cells incubated with ER-HNO (1 μM) for 15 min at 37 °C in acetonitrile-PBS buffer (0.2:99.8, v/v) at pH 7.2 displayed no intracellular fluorescence. In contrast, cells incubated with ER-HNO (1 μM) and then treated with AS for 30 min, showed strong intracellular fluorescence (Figure 3). These results confirm that ER-HNO is sufficiently bright and stable to be used as an imaging reagent for the detection of HNO uptake in live RAW macrophage cells through SIM imaging.

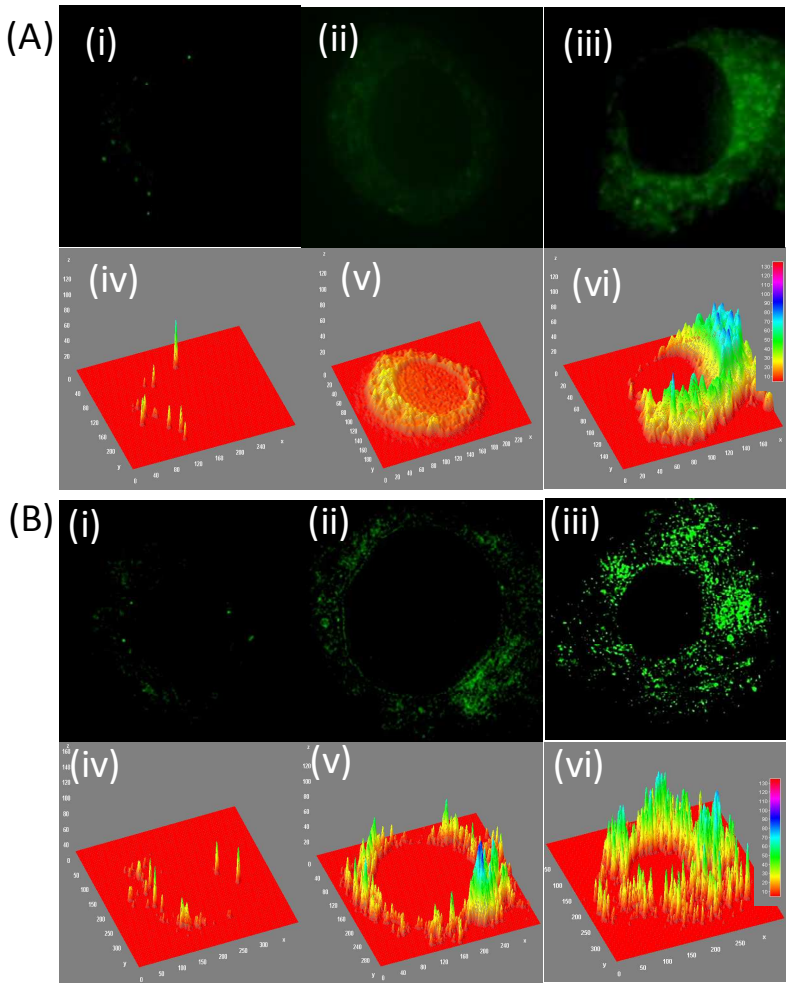

Figure 3. Comparison of Wide field (A) and SIM (B) Microscopic images of RAW 264.7 cells incubated with **ER-HNO** (i); Images of cells incubated with **ER-HNO** (1 μM) for 15 min and

then further exposed to (ii) 2 μM, (iii) 20 μM AS for 30 min at 37 ^{0}C (iv-vi) 3D intensity plot of image (i - iii). $\lambda_{Ext}/\lambda_{Em}$ = 568/586 nm.

To illustrate the resultant increased resolution of SIM compared to wide-field, a comparison of respective intensity/distance plots is also provided in Figure 3. The probe response to a wider range of concentrations (0 – 50 μM), showing clear dose-dependent emission intensity, is available in the SI. A close look at the images shown in Figure 3 suggests that the probe specifically localizes in the lipid dense region of RAW 264.7 cells. To explore this issue in more detail, co-localization studies were performed with the ER-specific reagent ER-Tracker Green, ER-TG.

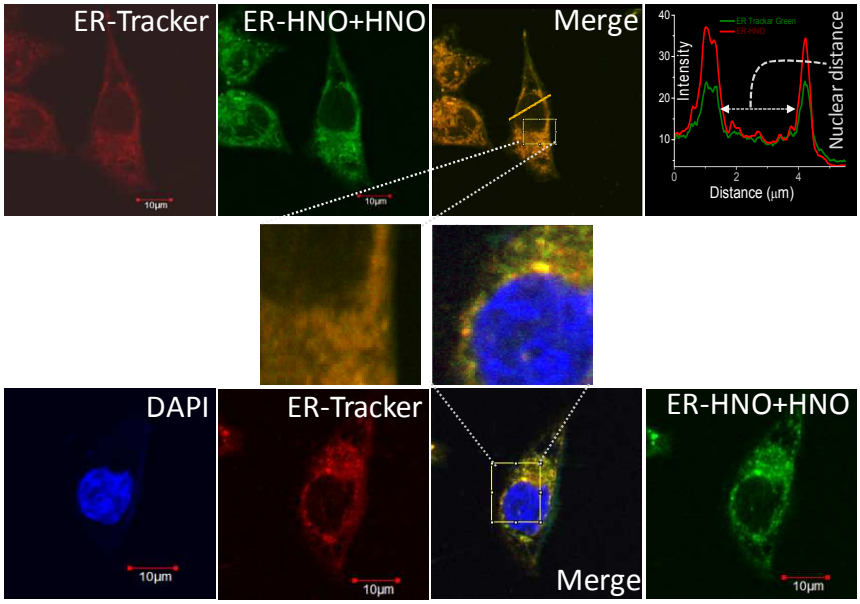

Figure 4. Colocalization studies of **ER-HNO** in presence of AS with DAPI and ER-Tracker Green in RAW 264.7 cells using CLSM imaging.

These studies revealed that emission from **ER-HNO**-treated cells in the presence of AS showed a very high Pearson's colocalization coefficient of 0.936 with ER-TG (SI); thus, **ER-HNO**

uniquely provides a method of mapping HNO in the ER region of RAW 264.7 cells. We then examined the potential of **ER-HNO** for dual colour SIM, D-SIM imaging.

Simultaneous use of different probes with complementary optical properties is often required for probing more than one intracellular biological process in real-time.

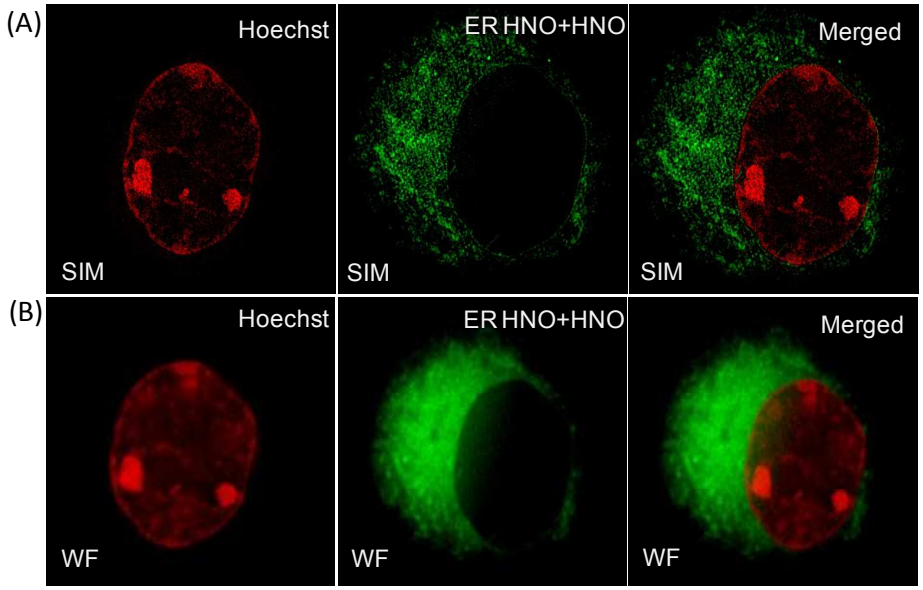

Figure 5. Dual Colour (A) SIM and (B) comparative Wide Field Fluorescence Microscopic images with Hoechst as the nuclear stain (Pseudo Colouring has been employed in all the Images) and **ER-HNO** as ER specific stain.

For this to be effected, the two probes used need to have complementary chemical and photophysical properties. As **ER-HNO** localizes in the ER, we looked to use it as a probe that is specific for a separate organelle with complementary optical properties. Since it is known that ROS generation in remote cell compartments can affect processes within the nucleus, as an initial proof of concept, we chose to use the common nuclear stain Hoechst 33342 (that groove binds to and visualizes chromatin DNA) as a complimentary probe in D-SIM imaging so as to simultaneously visualize HNO in the ER and also the nucleus. Figure 5 demonstrates that SIM

images of both HNO generation in the ER and chromatin morphology can be accomplished through this combination of ER-HNO and Hoechst 33342 staining. This provides a route to future studies in which the effects of a specific ROS generation within the ER has on the structure and function of the nucleus can be simultaneously probed. The feasibility of the reagent for biological *in-vivo* imaging was confirmed by imaging the digestive system of the small brine shrimp, Artemia nauplii, a small marine invertebrate as the model (Supporting Information). Hence, these results will facilitate future works aimed at investigating the effect of HNO mediated processes on whole cell morphology, which will be reported in forthcoming studies.

Conclusions

In Summary, **ER-HNO** exhibits high selectivity, excellent sensitivity and low cytotoxicity in the detection of HNO. The probe effectively detects HNO generated in the ER of live cells and its photophysical properties are compatible with its use in SIM and two colour SIM imaging, allowing more than one organelle to be imaged at superresolution. The possibility of using this reagent for *in-vivo* imaging application is demonstrated using Artemia, a small marine invertebrate, as the model.

Corresponding Authors

* E-mail: james.thomas@sheffield.ac.uk; a.das@csmcri.res.in

ACKNOWLEDGMENTS

A.D. acknowledges SERB (India) Grants (EMR/2016/001850 and JCB/2017/000004/SSC) and CSIR for funding. FA, NT and AHA acknowledge CSIR & UGC for their research fellowships. SS and JAT are grateful to the Imaging Life initiative of the University of Sheffield, and MRC

funding for the SIM facilities. FA, AD, and JAT are grateful to the GCRF for funding a visit by FA to Sheffield. Authors acknowledge the help extended by Mr. Nandaraj Taye of NCCS, Pune for the confocal experiment. Authors also thank Dr. Somuya Haldar and Dr. Sumit K. Pramanik in recoding the fluorescence images of *Artemia*.

ASSOCIATED CONTENT

Supporting Information is available free of charge on ACS Publication website.

Supporting Information is available free of charge on ACS Publication website. Details of synthesis, Characterization data of **ER-HNO**; spectral details photophysical studies. Imaging studies including detailed experimental procedure; Data Acquisition & data processing; Interference studies, ^{1}H NMR and ^{13}C NMR, MTT assay, details of SIM & Wide field imaging studies: General description, Sample preparation; and details of in vivo imaging in Artemia were provided in supporting information.

References:

(1) F. Doctorovich, P. J. Farmer, M. Marti, The Chemistry and Biology of Nitroxyl (HNO): 2nd edn, Elsevier, **2016**.

(2) Fukuto, J. M.; Bartberger, M. D.; Dutton, A. S.; Paolocci, N.; Wink, D. A.; Houk, K. N. *Chem. Res. Toxicol*. **2005**, *18*, 790–801.

(3) Hobbs, A. J.; Fukuto, J. M.; Ignarro, L. J. *Proc. Natl. Acad. Sci. U.S.A*. **1994**, *91*, 10992–10996.

(4) Favaloro, J. L.; Kemp-Harper, B. K. *Cardiovasc. Res*. **2007**, *73*, 587–596.

(5) Paolocci, N.; Jackson, M.; Lopez, B.; Miranda, K.; Tocchetti, C G.; Wink, D A.; Hobbs, A J.; Fukuto, J M. *Pharmacol. Ther*. **2007**, *113*, 442–458.

(6) Paolocci, N.; Katori, T.; Champion, H. C.; St. John, M. E.; Miranda, K. M.; Fukuto, J. M.; Wink, D. A.; Kass, D. A. *Proc. Natl. Acad. Sci. U.S.A* **2003**, *100*, 9 5537–5542.

(7) Augustyniak, A.; Skolimowski, J.; Błaszczyk, A. *Chem. Biol. Interact*. **2013**, *206*, 262–271.

(8) Keceli, G.; Toscano, J P. *Biochemistry* **2014**, *53*, 3689-98.

(9) Wrobel, A. T.; Johnstone, T. C.; Liang, A. D.; Lippard, S. J.; Fuentes, P. R. *J. Am. Chem. Soc*. **2014**, *136*, 4697-4705.

(10) Paolocci, N.; Saavedra, W.F.; Miranda, K. M.; Martignani, C.; Isoda, T.; Hare, J. M.; Espey, M. G.; Fukuto, J. M.; Feelisch, M.; Wink, D. A.; Kass, D. A. *Proc. Natl. Acad. Sci*. **2001**, *98*, 10463-10468.

(11) Switzer, C H.; Flores-Santana, W.; Mancardi, D.; Donzelli, S.; Basudhar, D.; Ridnour, L A.; et al. *BBA-Bioenergetics* **2009**, *1787*, 835-840.

(12) Miranda, K. M.; Paolocci, N.; Katori, T.; Thomas, D. D.; Ford, E.; Bartberger, M. D.; Espey, M. G.; Kass, D. A.; Feelisch, M.; Fukuto, J. M.; Wink, D. A. *Proc. Natl. Acad. Sci*. **2003**, *100*, 9196–9201.

(13) Bartberger, M. D.; Fukuto, J. M.; Houk, K. N. *Proc. Natl. Acad. Sci*. **2001**, *98*, 2194–2198.

(14) Shafirovich, V.; Lymar, S. V. *Proc. Natl. Acad. Sci., USA*. **2002**, *99*, 7340–7345.

(15) Miranda, K. M. *Coord. Chem. Rev*. **2005**, *249*, 433-455.

(16) Rosenthal, J.; Lippard, S. J. *J. Am. Chem. Soc*. **2010**, *132*, 5536-5537.

(17) Zhou, Y.; Liu, K.; Li, J.-Y.; Fang, Y.; Zhao, T.-C.; Yao, C.; *Org. Lett*. **2011**, *13*, 1290-1393.

(18) Suárez, S. A.; Bikiel, D. E.; Wetzler, D. E.; Martí, M. A.; Doctorovich, F. *Anal Chem*. **2013**, *85*, 10262-10269.

(19) Reisz, J. A.; Zink, C. N.; King, S. B. *J. Am. Chem. Soc*. **2011**, *133*, 11675-85.

(20) Reisz, J. A.; Klorig, E. B.; Wright, M.W.; King, S. B. *Org. Lett*. **2009**, *11*, 2719-2721.

(21) Kawai, K.; Ieda, N.; Aizawa, K.; Suzuki, T.; Miyata, N.; Nakagawa, H. *J. Am. Chem. Soc*. **2013**, *135*, 12690-12696.

(22) Jing, X.; Yu, F.; Chen, L. *Chem Commun*. **2014**, *50*, 14253-14256.

(23) Liu, C.; Wu, H.; Wang, Z.; Shao, C.; Zhu, B.; Zhang, X. *Chem Commun*. **2014**, *50*, 6013-6016.

(24) Mao, G.-J.; Zhang, X.-B.; Shi, X.-L.; Liu, H.-W.; Wu, Y.-X.; Zhou, L.-Y.; Tan, W.; Yu, R.-Q. *Chem. Commun*. **2014**, *50*, 5790-5792.

(25) Dong, B.; Song, X.; Kong, X.; Wang, C.; Zhang, N.; Lin, W. *J. Mater. Chem. B* **2017**, *5*, 5218—5224.

(26) Ren, M.; Deng, B.; Zhou, K.; Wang, J.-Y.; Kong, X.; Lin, W. *J. Mater. Chem. B* **2017**, *5*, 1954—1961.

(27) Zheng, K.; Lin, W.; Cheng, D.; Chen, H.; Liu, Y.; Liu, K. *Chem. Commun*. **2015**, *51*, 5754—5757.

(28) Ping, L.; Xiao-Yue, H.; Fa-Biao, Y.; Ling-Xin, C. *Chin. J. Anal. Chem*. **2015**, *43*, 1829–1836.

(29) Liu, P.; Jing, X.; Yu, F.; Lvb, C.; Chen, L. *Analyst* **2015**, 140, 4576-4583.

(30) Zhang, H.; Liu, R.; Tan, Y.; Xie, W. H.; Lei, H.; Cheung, H.-Y.; Sun, H. *ACS Appl. Mater. Interfaces* **2015**, *7*, 5438-5443.

(31) Rosenthal, J.; Lippard, S. J. *J. Am. Chem. Soc*. **2010**, *132*, 5536-5537.

(32) Zheng, K.; Lin, W.; Cheng, D.; Chen, H.; Liu, Y.; Liu, K. *Chem. Commun*. **2015**, *51*, 5754-5757.

(33) Thomas, J. A. *Chem. Soc. Rev*. **2015**, 44, 4494—4500.

(34) Wegel1, E.; Göhler, A.; Lagerholm, B. C.; Wainman, A.; Uphoff, S.; Kaufmann, R.; Dobbie, I. M. *Sci. Rep*. **2016**, doi:10.1038/srep27290.

(35) Van de Linde, S.; Heilemann, M.; Sauer, M. *Annu. Rev. Phys. Chem*. **2012**, *63*, 519–540.

(36) Ali, F., Anila, H. A.; Taye, N.; Gonnade, R. G.; Chattopadhyay, S.; Das, A. *Chem. Commun.* **2015**, *51*, 16932—16935.

(37) Dong, B.; Zheng ,K.; Tanga, Y.; Lin, W.; *J. Mater. Chem. B* **2016**, *4*, 1263—1269.

(38) Sunwoo, K.; Bobba, K. N.; Lim, J.-Y.; Park, T.; Podder, A.; Heo, J. S.; Lee, S. G.; Bhuniya, S.; Kim, J. S.; *Chem. Commun*. **2017**, *53*, 1723-1726.

(39) Rivera-Fuentes, P.; Lippard, S. J.; *Acc. Chem. Res*. **2015**, *48*, 2927-2934.

(40) Miranda, K M.; Nagasawa, H T.; Toscano, J P. *Curr Top Med Chem*. **2005**, *5*, 649-664.

TOC